

NLO QCD Corrections to Inclusive Charmonium and B_c Meson Production in W^+ Decays

Zi-Qiang Chen^{1†}, Hao Yang^{1‡} and Cong-Feng Qiao^{1,2*}

¹ *School of Physics, University of Chinese Academy of Science,*

Yuquan Road 19A, Beijing 10049

² *CAS Key Laboratory of Vacuum Physics, Beijing 100049, China*

Abstract

We calculate the next-to-leading order (NLO) quantum chromodynamics (QCD) corrections to inclusive processes $W^+ \rightarrow J/\psi(\eta_c) + c + \bar{s} + X$ and $W^+ \rightarrow B_c(B_c^*) + b + \bar{s} + X$ in the framework of nonrelativistic QCD (NRQCD) factorization formalism. Result indicates that the NLO corrections are significant, and the uncertainties in theoretical predictions with NLO corrections are greatly reduced. The charmonium and B_c meson yielding rates at the Large Hadron Collider (LHC) are given.

PACS numbers: 12.38.Bx, 12.39.Jh, 13.38.Be, 14.40.Pq

[†] chenziqiang13@mails.ucas.ac.cn

[‡] yanghao174@mails.ucas.ac.cn

* qiaocf@ucas.ac.cn, corresponding author

I. INTRODUCTION

In the standard model (SM), the W boson mass is generated through the electroweak spontaneous breaking mechanism. Precise measurement of W boson mass and its decay width turns out to be a unique test of the SM and hence a probe for new physics. At the Large Hadron Collider (LHC), a huge number of W bosons are produced and recorded, which enables the research on W physics feasible and meaningful.

Heavy quarkonium and as well B_c meson production keeps on being an interesting and hot topic to study in high energy physics for decades, which may enrich our knowledge on the properties of quarkonium and the nature of perturbative QCD. Note, hereafter for simplicity the B_c represents for both scalar B_c and vector B_c^* unless specifically mentioned. Based on the nonrelativistic QCD (NRQCD) factorization formalism [1], direct hadroproduction of quarkonium and B_c meson was studied extensively [2–12]. In addition to the direct production, indirect production also stands as an independent and important source for those double-heavy mesons. The quarkonium and B_c meson production through top quark [13] and Z_0 decays [14–16] had been investigated at up to the next-to-leading order (NLO) accuracy. For indirect quarkonium and B_c in W decays, the leading order (LO) analyses were performed in Refs.[17, 18]. It turned out that the theoretical uncertainties at LO are very large, which suggests, and was partly confirmed, that the higher order QCD corrections in charmonium and B_c productions are usually very important, even crucial sometimes, for the sake of phenomenological use. To this end, we calculate in this work the NLO QCD corrections to the inclusive charmonium and B_c production in W^+ decays.

The rest of the paper is organized as follows. In section II we present the LO calculation of W^+ decay to charmonium and B_c mesons. In section III, some technical details in the calculation of NLO corrections are given. In section IV, the numerical evaluation for concerned processes is performed at NLO QCD accuracy. The last section is remained for summary and conclusions.

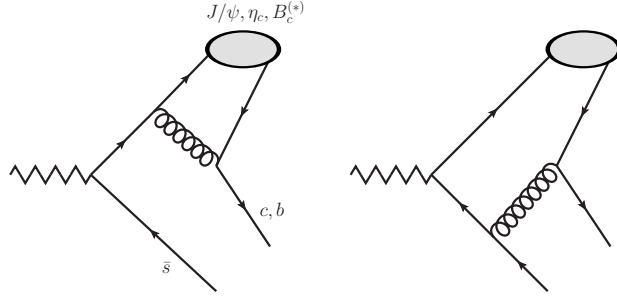


FIG. 1: The LO Feynman diagrams for charmonium and B_c meson production in W^+ decays.

II. THE LO DECAY WIDTH

At the LO in α_s , inclusive charmonium and B_c meson production through W^+ decays are described by the processes

$$\begin{aligned} W^+(p_W) &\rightarrow J/\psi(\eta_c)(p_H) + c(p_Q) + \bar{s}(p_s), \\ W^+(p_W) &\rightarrow B_c(B_c^*)(p_H) + b(p_Q) + \bar{s}(p_s) \end{aligned} \quad (1)$$

as shown in Fig.1. The initial and final state particles are on the mass shell: $p_W^2 = m_W^2$, $p_H^2 = m_H^2$, $p_Q^2 = m_Q^2$ and $p_s^2 = 0$. We also introduce the Mandelstam variables: $s_1 = (p_H + p_Q)^2$, $s_2 = (p_H + p_s)^2$. The CKM-suppressed processes, such as $W^+ \rightarrow B_c(B_c^*) + c + \bar{c}$, are not included in our calculation. The amplitudes of these processes are suppressed at least by a Wolfenstein parameter λ . Taking $\lambda \sim \alpha_s(2m_c)$, the suppress factor for decay width can be estimated as $\mathcal{O}(\alpha_s^2)$, which means that the contribution from these processes are less significant than the NLO corrections.

At the leading order of the relative velocity expansion, it is legitimate to take $p_c = p_{\bar{c}}$, $m_H = 2m_c$ for charmonium production and $p_c = \frac{m_c}{m_b} p_{\bar{b}}$, $m_H = m_b + m_c$ for B_c production. The spin projection operator has the form

$$\Pi(n) = \frac{1}{2\sqrt{m_H}} \epsilon(n) (\not{p}_H + m_H) \otimes \left(\frac{1_c}{\sqrt{N_c}} \right), \quad (2)$$

where $\epsilon(^1S_0) = \gamma_5$ and $\epsilon(^3S_1) = \not{\epsilon}$. The decay width at LO reads:

$$\Gamma_{\text{born}} = \frac{|\Psi_H(0)|^2}{2m_W} \frac{1}{3} \int \sum |\mathcal{M}_{\text{born}}|^2 d\text{PS}_3. \quad (3)$$

Here, \sum sums over the polarizations and colors of the initial and final particles, $\frac{1}{3}$ comes from the spin average of the initial W^+ boson, $d\text{PS}_3$ stands for the three-body phase space, which can be expressed as

$$\int d\text{PS}_3 = \frac{1}{32\pi^3} \int_{m_H}^{E_H^+} dE_H \int_{E_s^-}^{E_s^+} dE_s, \quad (4)$$

in the rest frame of W^+ . Here, E_H and E_s represent the energy of final state hadron and s quark respectively. The upper and lower bounds of above integration are

$$E_H^+ = \frac{m_W^2 + m_H^2 - m_Q^2}{2m_W},$$

$$E_s^\pm = \frac{1}{2} \left(1 - \frac{m_Q^2}{M_{Qs}^2} \right) \left(m_W - E_H \pm \sqrt{E_H^2 - m_H^2} \right). \quad (5)$$

with

$$M_{Qs}^2 = m_W^2 + m_H^2 - 2m_W E_H. \quad (6)$$

III. THE NLO CORRECTIONS

At the NLO, the W^+ boson decay to charmonium and $B_c(B_c^*)$ meson include the virtual and real corrections of $W^+ \rightarrow J/\psi(\eta_c) + c + \bar{s}$ and $W^+ \rightarrow B_c(B_c^*) + b + \bar{s}$ processes. For η_c production, new subprocess $W^+ \rightarrow \eta_c + u + \bar{d} + g$ should also be included. In the computation of NLO corrections, the conventional dimensional regularization with $D = 4 - 2\epsilon$ is adopted to regularize the ultraviolet (UV) and infrared (IR) divergences. The method proposed in [19, 20] is used to deal with the D dimensions γ_5 trace.

In the calculation, the package FeynArts [21] is used to generate Feynman diagrams; FeynCalc [22, 23] and FORM [24, 25] are used to perform algebraic calculation; FIRE [26, 27] is employed to reduce the Feynman integrals into the master integrals (A_0, B_0, C_0, D_0); With the help of Ref.[28] and Package-X [29], the master integrals are calculated analytically, and the results are checked by LoopTools [30]; The numerical phase space integration is performed by CUBA[31].

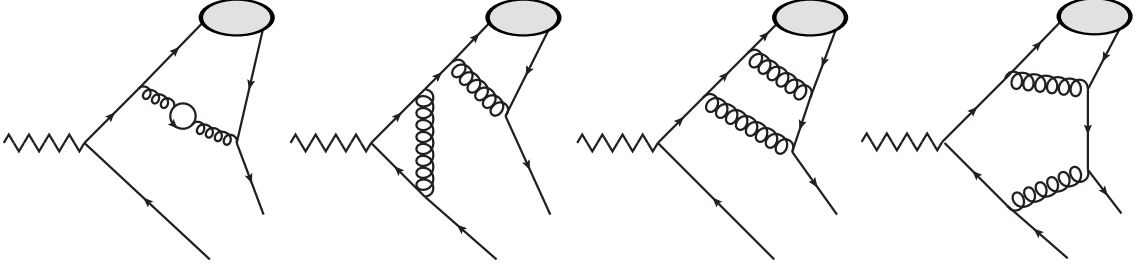


FIG. 2: Typical Feynman diagrams in virtual corrections.

A. Virtual corrections

Typical Feynman diagrams in virtual corrections are shown in Fig.2. The contribution from virtual corrections can be formulated as

$$\Gamma_{\text{virtual}} = \frac{|\Psi_H(0)|^2}{2m_W} \frac{1}{3} \int \sum 2\text{Re}(\mathcal{M}_{\text{virtual}} \mathcal{M}_{\text{born}}^*) d\text{PS}_3. \quad (7)$$

Here, $\text{Re}(\mathcal{M}_{\text{virtual}} \mathcal{M}_{\text{born}}^*)$ contains both UV and IR singularities. Since we set $p_c = p_{\bar{c}}$ and $p_c = \frac{m_c}{m_b} p_{\bar{b}}$ before the calculation of Feynman integrals, the Coulomb singularity are not expected to appear in our calculation [32].

The UV singularities are removed by renormalization. For the renormalization of heavy quark field (Z_2), heavy quark mass (Z_m) and light quark field (Z_l), we take the on-shell (OS) scheme; for the renormalization of gluon field (Z_3) and strong coupling constant (Z_g), the modified minimal-subtraction ($\overline{\text{MS}}$) schemes are used:

$$\begin{aligned} \delta Z_2^{\text{OS}} &= -C_F \frac{\alpha_s}{4\pi} \left[\frac{1}{\epsilon_{\text{UV}}} + \frac{2}{\epsilon_{\text{IR}}} - 3\gamma_E + 3 \ln \frac{4\pi\mu^2}{m_Q^2} + 4 \right], \\ \delta Z_m^{\text{OS}} &= -3C_F \frac{\alpha_s}{4\pi} \left[\frac{1}{\epsilon_{\text{UV}}} - \gamma_E + \ln \frac{4\pi\mu^2}{m_Q^2} + \frac{4}{3} \right], \\ \delta Z_l^{\text{OS}} &= -C_F \frac{\alpha_s}{4\pi} \left[\frac{1}{\epsilon_{\text{UV}}} - \frac{1}{\epsilon_{\text{IR}}} \right], \\ \delta Z_3^{\overline{\text{MS}}} &= \frac{\alpha_s}{4\pi} (\beta_0 - 2C_A) \left[\frac{1}{\epsilon_{\text{UV}}} - \gamma_E + \ln(4\pi) \right], \\ \delta Z_g^{\overline{\text{MS}}} &= -\frac{\beta_0}{2} \frac{\alpha_s}{4\pi} \left[\frac{1}{\epsilon_{\text{UV}}} - \gamma_E + \ln(4\pi) \right]. \end{aligned} \quad (8)$$

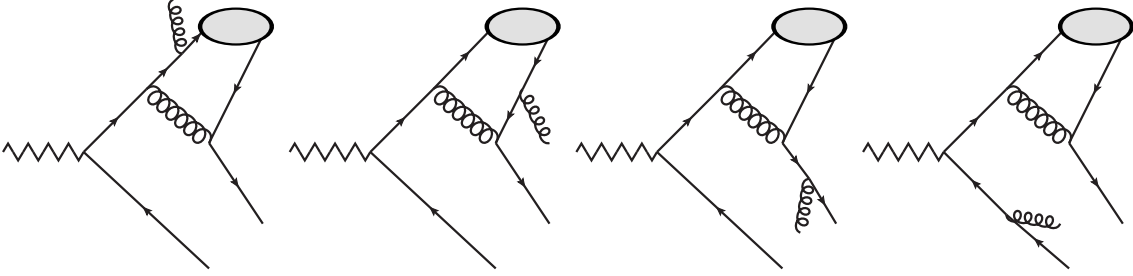


FIG. 3: Typical Feynman diagrams in real corrections.

Here, μ is the renormalization scale, γ_E is the Euler's constant; $\beta_0 = (11/3)C_A - (4/3)T_f n_f$ is the one-loop coefficient of QCD beta function, n_f is the number of active quarks; $C_A = 3$, $C_F = 4/3$ and $T_F = 1/2$ are color factors. Note, final result is independent of δZ_3 , because terms proportional to δZ_3 from vertex correction cancel with that from selfenergy correction.

In virtual corrections, the IR singularities arise when the gluon connecting two on shell partons is soft or collinear to final \bar{s} quark. Due to $p_c = p_{\bar{c}}$ or $p_c = \frac{m_c}{m_b} p_{\bar{b}}$, parts of IR singularities cancel each other [1]. The remaining are canceled by the real corrections according to the Kinoshita-Lee-Nauenberg theorem [33, 34].

B. Real corrections

Typical Feynman diagrams in real corrections are shown in Fig.3. In the calculation of the real corrections, the phase space slicing method [35] is adopted to separate the IR singularities. By introducing soft cut δ_s and collinear cut δ_c , the phase space can be separated into three regions:

- Soft: $p_g^0 < \frac{m_W}{2} \delta_s$;
- Hard collinear: $p_g^0 > \frac{m_W}{2} \delta_s$, $M_{sg}^2 < m_W^2 \delta_c$;
- Hard non-collinear: $p_g^0 > \frac{m_W}{2} \delta_s$, $M_{sg}^2 > m_W^2 \delta_c$.

Here, $M_{sg} = (p_s + p_g)^2$ is the invariant mass of \bar{s} and g system. Then the real corrections can be written as

$$\Gamma_{\text{real}} = \Gamma_{\text{real}}^{\text{S}} + \Gamma_{\text{real}}^{\text{HC}} + \Gamma_{\text{real}}^{\text{HNC}}, \quad (9)$$

where the superscripts “S”, “HC”, “HNC” represent the “soft”, “hard collinear”, “hard non-collinear” region respectively.

According to Ref.[35], the contributions from soft part and hard collinear part reads

$$\begin{aligned} \Gamma_{\text{real}}^{\text{S}} &= \Gamma_{\text{born}} C_F \frac{\alpha_s}{2\pi} \frac{\Gamma(1-\epsilon)}{\Gamma(1-2\epsilon)} \left(\frac{4\pi\mu^2}{m_W^2} \right)^\epsilon \frac{1}{\delta_s^{2\epsilon}} \\ &\quad \times \left[\frac{1}{\epsilon^2} + \frac{1}{\epsilon} \left(1 - \ln \frac{m_W^2}{m_Q^2} - 2 \ln \frac{m_H^2 + m_W^2 - s_1 - s_2}{m_W^2 - s_1} \right) + \text{finite} \right], \\ \Gamma_{\text{real}}^{\text{HC}} &= \Gamma_{\text{born}} C_F \frac{\alpha_s}{2\pi} \frac{\Gamma(1-\epsilon)}{\Gamma(1-2\epsilon)} \left(\frac{4\pi\mu^2}{m_W^2} \right) \\ &\quad \times \left[\frac{1}{\epsilon} \left(2 \ln \frac{m_W^2 \delta_s}{m_W^2 - s_1} + \frac{3}{2} \right) - \frac{3}{2} \ln \delta_c - 2 \ln \delta_c \ln \frac{m_W^2 \delta_s}{m_W^2 - s_1} \right. \\ &\quad \left. - \left(\ln \frac{m_W^2 \delta_s}{m_W^2 - s_1} \right)^2 - \frac{2\pi^2 - 21}{6} \right]. \end{aligned} \quad (10)$$

In the case of hard non-collinear part, the decay width reads

$$\Gamma_{\text{real}}^{\text{HNC}} = \frac{|\Psi_H(0)|^2}{2m_W} \frac{1}{3} \int^{\text{HNC}} \sum |\mathcal{M}_{\text{real}}|^2 d\text{PS}_4, \quad (11)$$

where the four-body phase space $d\text{PS}_4$ with cut can be written as

$$\begin{aligned} \int^{\text{HNC}} d\text{PS}_4 &= \frac{1}{512\pi^6} \int_{m_H}^{E_H^+} dE_H \int_{\sqrt{\delta_c} m_W}^{M_{sg}^+} dM_{sg} \int_{E_{sg}^-}^{E_{sg}^+} dE_{sg} \frac{M_{sg}}{\sqrt{E_{sg}^2 - M_{sg}^2}} \\ &\quad \int_{\max(E_g^-, \delta_s m_W/2)}^{E_g^+} dE_g \Theta(E_g^+ - \delta_s m_W/2) \int_0^{2\pi} d\eta_{sg}, \end{aligned} \quad (12)$$

with

$$\begin{aligned} E_H^+ &= \frac{m_W^2 + m_H^2 - (m_Q + \sqrt{\delta_c} m_W)^2}{2m_W}, \\ M_{csg} &= \sqrt{m_W^2 + m_H^2 - 2m_W E_\psi}, \\ M_{sg}^+ &= M_{csg} - m_Q, \\ E_{sg}^\pm &= \frac{1}{4m_W M_{csg}^2} \left[(M_{csg}^2 - m_Q^2 + M_{sg}^2)(m_W^2 - m_H^2 + M_{csg}^2) \right. \\ &\quad \left. \pm \sqrt{(M_{csg}^2 - m_Q^2 + M_{sg}^2)^2 - 4m_W^2 M_{csg}^2} \right] \end{aligned}$$

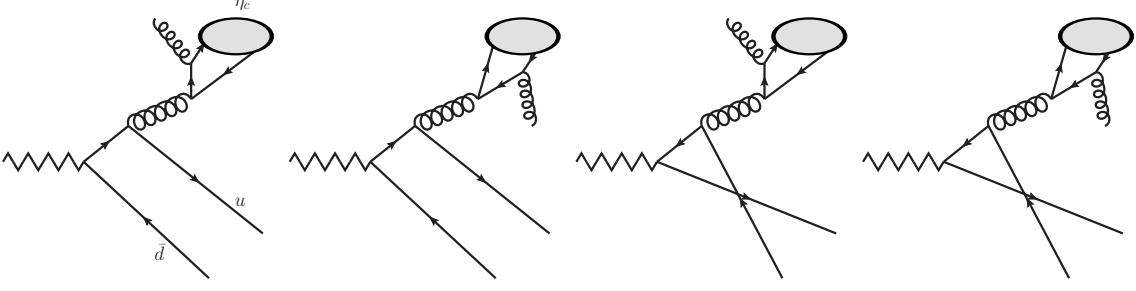


FIG. 4: Feynman diagrams of $W^+ \rightarrow \eta_c + u + \bar{d} + g$ process.

$$\pm \sqrt{\lambda(M_{csg}^2, m_Q^2, M_{sg}^2) \lambda(m_W^2, m_H^2, M_{csg}^2)} \Big],$$

$$E_g^\pm = \frac{1}{2} \left(E_{sg} \pm \sqrt{E_{sg}^2 - M_{sg}^2} \right), \quad (13)$$

where $\lambda(s, m_a^2, m_b^2) = [s - (m_a + m_b)^2][s - (m_a - m_b)^2]$, and $\Theta(x)$ is the unit step function which return 1 when $x > 0$ and 0 for other case. After summing up these three parts, their dependence on technical cut are eliminated as expected.

For the subprocess $W^+ \rightarrow \eta_c + u + \bar{d} + g$, there are 4 diagrams, as shown in Fig.4. The IR singularities are eliminated after summing all the amplitude square parts. The decay width can be calculated directly in 4 dimensions as $\Gamma_{\text{real}}^{\text{HNC}}$.

IV. NUMERICAL RESULTS

For the numerical calculation, following input parameters are used

$$m_W = 80.399 \text{ GeV}, \quad m_c = 1.5 \pm 0.1 \text{ GeV}, \quad m_b = 4.9 \pm 0.2 \text{ GeV}, \quad \alpha = 1/137.065,$$

$$\sin^2 \theta_W = 0.2312, \quad |\Psi_{J/\psi}^{\text{LO}}(0)|^2 = \frac{0.528}{4\pi} \text{ GeV}^3, \quad |\Psi_{J/\psi}^{\text{NLO}}(0)|^2 = \frac{0.903}{4\pi} \text{ GeV}^3,$$

$$\Psi_{\eta_c}(0) = \Psi_{J/\psi}(0), \quad |\Psi_{B_c}(0)|^2 = |\Psi_{B_c^*}(0)|^2 = \frac{1.642}{4\pi} \text{ GeV}^3. \quad (14)$$

Here, θ_W is the Weinberg angle. The J/ψ wave function at the origin is extracted from its leptonic width:

$$\Gamma(J/\psi \rightarrow e^+ e^-) = \frac{16\pi\alpha^2}{9m_c^2} |\Psi_{J/\psi}(0)|^2 \left(1 - 4C_F \frac{\alpha_s}{\pi} \right), \quad (15)$$

with $\Gamma(J/\psi \rightarrow e^+e^-) = 5.55 \text{ keV}$ [36]. The B_c wave function is estimated by using the Buchmueller-Tye potential [37]. The two-loop strong coupling of

$$\frac{\alpha_s(\mu)}{4\pi} = \frac{1}{\beta_0 L} - \frac{\beta_1 \ln L}{\beta_0^3 L^2} \quad (16)$$

is employed in the NLO calculation, in which, $L = \ln(\mu^2/\Lambda_{\text{QCD}}^2)$, $\beta_0 = (11/3)C_A - (4/3)T_F n_f$, $\beta_1 = (34/3)C_A^2 - 4C_F T_F n_f - (20/3)C_A T_F n_f$. We take $n_f = 4$, $\Lambda_{\text{QCD}} = 292 \text{ MeV}$ for J/ψ and η_c production; $n_f = 5$, $\Lambda_{\text{QCD}} = 210 \text{ MeV}$ for B_c and B_c^* production.

The NLO decay width can be expressed as

$$\Gamma_H^{\text{NLO}}(\mu) = \frac{\alpha\alpha_s(\mu)^2}{\sin^2\theta_W} |\Psi_H(0)|^2 \left(A_H + \frac{\alpha_s(\mu)}{\pi} \left(B_H + A_H C_H \ln \frac{\mu^2}{m_W^2} \right) \right), \quad (17)$$

where $C_H = 25/6$ for $W^+ \rightarrow J/\psi(\eta_c) + c + \bar{s}$, $C_H = 0$ for $W^+ \rightarrow \eta_c + u + \bar{d} + g$, $C_H = 23/6$ for $W^+ \rightarrow B_c(B_c^*) + b + \bar{s}$. The parameters A_H and B_H are independent of μ , their values at different heavy quark mass are shown in Tab.I.

TABLE I: The parameters A_H and B_H in Eq.17. The units of heavy quark mass and A_H are suppressed for brevity, which are GeV and GeV^{-2} respectively.

$W^+ \rightarrow H q_i \bar{q}_j$	$m_c = 1.4, m_b = 4.7$		$m_c = 1.5, m_b = 4.9$		$m_c = 1.6, m_b = 5.1$	
	A_H	B_H	A_H	B_H	A_H	B_H
$W^+ \rightarrow J/\psi c \bar{s}$	1.04	30.5	0.846	24.2	0.695	19.6
$W^+ \rightarrow \eta_c c \bar{s}$	1.01	35.0	0.818	27.7	0.673	22.4
$W^+ \rightarrow \eta_c u \bar{d} g$	0	4.01	0	3.04	0	2.46
$W^+ \rightarrow B_c b \bar{s}$	0.0230	0.661	0.0201	0.569	0.0177	0.495
$W^+ \rightarrow B_c^* b \bar{s}$	0.0198	0.474	0.0173	0.408	0.0152	0.355

The decay widths are as presented in Tab.II. The theoretical uncertainties are estimated by varying the value of heavy quark mass and normalization scale: $m_c \in [1.4, 1.6] \text{ GeV}$, $m_b \in [4.7, 5.1] \text{ GeV}$, $\mu \in [m_H, \frac{m_W^2 + m_H^2 - m_Q^2}{2m_W}]$. According to Ref.[36], total decay width for W^+ boson is about 2.195 GeV, the corresponding branching fractions are then shown in Tab.III. With NLO corrections, the theoretical uncertainties induced

by heavy quark mass and normalization scale are greatly suppressed as expected. The decay widths versus running renormalization scale at $m_c = 1.5$ GeV and $m_b = 4.9$ GeV are exhibited in Fig.5.

TABLE II: Decay widths of W^+ inclusive decay to charmonium and $B_c(B_c^*)$ meson. The upper bound corresponding to $m_c = 1.4$ GeV, $m_b = 4.7$ GeV and $\mu = m_H$, and the lower bound to $m_c = 1.6$ GeV, $m_b = 5.1$ GeV and $\mu = \frac{m_W^2 + m_H^2 - m_Q^2}{2m_W}$.

	$\Gamma(J/\psi c\bar{s})(\text{keV})$	$\Gamma(\eta_c c\bar{s})(\text{keV})$	$\Gamma(\eta_c u\bar{d}g)(\text{keV})$	$\Gamma(B_c b\bar{s})(\text{keV})$	$\Gamma(B_c^* b\bar{s})(\text{keV})$
LO	21.6 \sim 154.0	20.9 \sim 149.0	-	1.77 \sim 5.62	1.53 \sim 4.82
NLO	48.3 \sim 163.7	51.8 \sim 220.6	3.61 \sim 45.9	2.52 \sim 5.82	1.96 \sim 4.04

TABLE III: Branching fractions of W^+ inclusive decay to charmonium and $B_c(B_c^*)$ meson. The upper bound corresponding to $m_c = 1.4$ GeV, $m_b = 4.7$ GeV and $\mu = m_H$, and the lower bound to $m_c = 1.6$ GeV, $m_b = 5.1$ GeV and $\mu = \frac{m_W^2 + m_H^2 - m_Q^2}{2m_W}$.

	$\text{Br}(J/\psi c\bar{s})(10^{-5})$	$\text{Br}(\eta_c c\bar{s})(10^{-5})$	$\text{Br}(\eta_c u\bar{d}g)(10^{-5})$	$\text{Br}(B_c b\bar{s})(10^{-5})$	$\text{Br}(B_c^* b\bar{s})(10^{-5})$
LO	0.984 \sim 7.02	0.952 \sim 6.79	-	0.0806 \sim 0.256	0.0697 \sim 0.220
NLO	2.20 \sim 7.46	2.36 \sim 10.05	0.164 \sim 2.09	0.115 \sim 0.265	0.0893 \sim 0.184

The energy distribution of charmonium and $B_c(B_c^*)$ meson are shown in Fig.6. It can be seen from Fig.6(b) that the η_c production rate are largely enhanced at small energy region. This enhancement comes from the diagrams similar to Fig.4, except u and \bar{d} are replaced by c and \bar{s} . The contribution from the gluon propagator can be estimated as:

$$\int_{-1}^1 d\cos\theta_{ng} \frac{1}{(4m_c^2 + 2E_\eta E_g - 2|\vec{p}_\eta|E_g \cos\theta_{ng})^2} \sim \frac{1}{E_g E_\eta + E_g^2 + m_c^2}, \quad (18)$$

which explain the enhancement at small energy region.

The instantaneous luminosity of LHC reach $2.06 \times 10^{34} \text{ cm}^{-2}\text{s}^{-1}$ in 2017 [38]. The production cross section of W^+ boson at the LHC can be estimated to be 100 nb [39], then the number of W^+ events per year is about 6.5×10^{10} . Hence we can

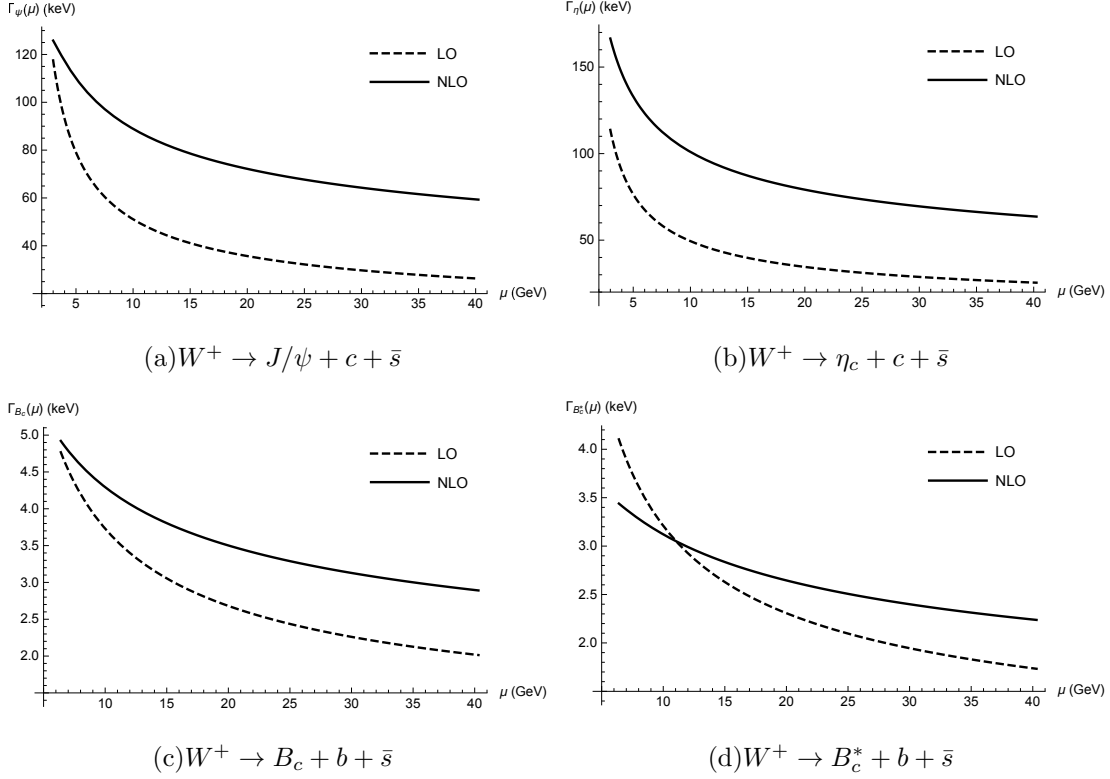


FIG. 5: The LO (dashed line) and NLO (solid line) decay widths versus running renormalization scale.

obtain about $(1.43 \sim 4.85) \times 10^6$ J/ψ events, $(1.64 \sim 7.89) \times 10^6$ η_c events and $(1.33 \sim 2.92) \times 10^5$ B_c events per year. Here, the B_c^* feed-down to B_c is taken into account. In experiment, the B_c meson can be fully reconstructed through $B_c \rightarrow J/\psi \pi^+$ decay, whose branching fraction is about 0.5% [40]. According to [36], the branching ratio $B_r(J/\psi \rightarrow l^+ l^- (l = e, \mu)) = 12\%$, $B_r(\eta_c \rightarrow p \bar{p}) = 0.15\%$, then the numbers of J/ψ , η_c and B_c meson candidates per year are $(1.72 \sim 5.82) \times 10^5$, $(2.46 \sim 11.8) \times 10^3$ and $80 \sim 175$ respectively.

V. SUMMARY AND CONCLUSIONS

In this work we calculate the decay widths of W^+ to J/ψ , η_c and $B_c(B_c^*)$ mesons at the NLO QCD accuracy within the NRQCD factorization framework. The theoretical

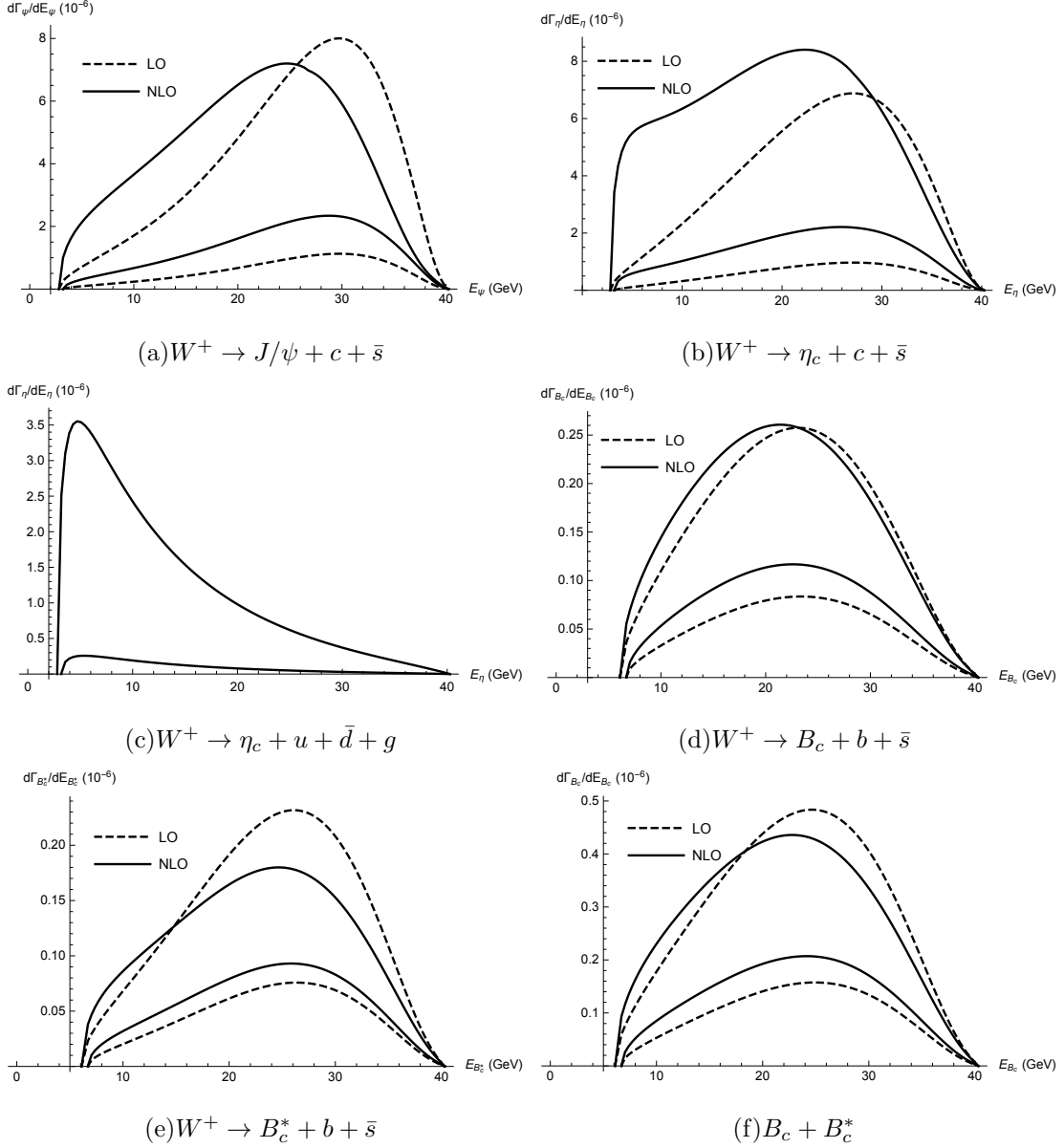


FIG. 6: The charmonium and $B_c(B_c^*)$ meson energy distribution in W^+ decay. The LO and NLO results are represented by double-dashed and double-solid lines, referring to the upper and lower bounds of uncertainties, respectively.

uncertainties are estimated by varying the value of heavy quark mass and renormalization scale. Considering there are copious W data at the LHC, our results are hopefully to be tested in experiment.

Numerical calculation shows that the NLO corrections are significant, and the uncertainties in theoretical predictions with NLO corrections are greatly reduced. Since B_c^* almost all decays to B_c , assuming B_c is reconstructed through $B_c \rightarrow J/\psi \pi^+$, J/ψ is reconstructed through $J/\psi \rightarrow l^+ l^-$ ($l = e, \mu$), η_c is reconstructed through $\eta_c \rightarrow p \bar{p}$, the numbers of J/ψ , η_c and B_c meson candidates per year may reach $(1.72 \sim 5.82) \times 10^5$, $(2.46 \sim 11.8) \times 10^3$ and $80 \sim 175$ respectively at the LHC 2017 luminosity.

Note added: when this work was finished and the manuscript was finalizing, there appears a study on the web about the $B_c(B_c^*)$ meson production in W^+ decay with the NLO QCD corrections [41]. We numerically compared our results with that paper, and find that by taking the same inputs we can reproduce the Table I results there¹.

Acknowledgments

This work was supported in part by the Ministry of Science and Technology of the Peoples' Republic of China(2015CB856703) and by the National Natural Science Foundation of China(NSFC) under the Grants 11975236, 11635009, and 11375200.

-
- [1] G. T. Bodwin, E. Braaten and G. P. Lepage, Phys. Rev. D 51, 1125 (1995); 55, 5853(E) (1997).
 - [2] J. M. Campbell, F. Maltoni and F. Tramontano, Phys. Rev. Lett 98, 252002 (2007).
 - [3] B. Gong and J. X. Wang, Phys. Rev. Lett 100, 232001 (2008).
 - [4] Y. Q. Ma, K. Wang and K. T. Chao, Phys. Rev. Lett 106, 042002 (2011).
 - [5] M. Butenschoen and B. A. Kniehl, Phys. Rev. Lett. 106, 022003 (2011).
 - [6] M. Butenschoen, Z. G. He and B. A. Kniehl, Phys. Rev. Lett. 144, 092004 (2015).
 - [7] H. Han, Y. Q. Ma, C. Meng, H. S. Shao and K. T. Chao, Phys. Rev. Lett. 144, 092005

¹ In Ref.[41], the two-loop α_s is used both in the LO and NLO calculation, while in our calculation, the one-loop and two-loop α_s are employed respectively.

- (2015).
- [8] H. F. Zhang, Z. Sun, W. L. Sang and R. Li, Phys. Rev. Lett. 144, 092006 (2015).
 - [9] C. H. Chang and Y. Q. Chen, Phys. Rev. D 48, 4086 (1993).
 - [10] C. H. Chang, Y. Q. Chen, G. P. Han and H. T. Jiang, Phys. Letts. B 364, 78 (1995).
 - [11] K. Kolodziej, A. Leike and R. Ruckl, Phys. Letts. B 355, 337 (1995).
 - [12] A. V. Berezhnoy, A. K. Likhoded and M. V. Shevlyagin, Phys. Atom. Nucl. 58, 672 (1995).
 - [13] P. Sun, L. P. Sun and C. F. Qiao, Phys. Rev. D 81, 114035 (2010).
 - [14] R. Li and J. X. Wang, Phys. Rev. D 82, 054006 (2010).
 - [15] C. F. Qiao, L. P. Sun and R. L. Zhu, JHEP 1108, 131 (2011).
 - [16] J. Jiang, L. B. Chen and C. F. Qiao, Phys. Rev. D 91, 034033 (2015).
 - [17] C. F. Qiao, L. P. Sun, D. S. Yang and R. L. Zhu, Eur. Phys. J. C 71, 1766 (2011).
 - [18] Q. L. Liao, X. G. Wu, J. Jiang, Z. Yang and Z. Y. Fang, Phys. Rev. D 85, 014032 (2012).
 - [19] D. Kreimer, Phys. Lett. B 237, 59 (1990).
 - [20] J. G. Korner, D. Kreimer and K. Schilcher, Z. Phys. C 54, 503 (1992).
 - [21] T. Hahn, Comput. Phys. Commun 140, 418 (2001).
 - [22] R. Mertig, M. Bohm and A. Denner, Comput. Phys. Commun 64, 345 (1991).
 - [23] V. Shtabovenko, R. Mertig and F. Orellana, Comput. Phys. Commun 207, 432 (2016).
 - [24] J. A. M. Vermaseren, Nucl. Phys. B (Proc. Suppl.) 183, 19 (2008).
 - [25] J. Kuipers, T. Ueda, J. A. M. Vermaseren and J. Vollinga, Comput. Phys. Commun 184, 1453 (2013).
 - [26] A. V. Smirnov, JHEP 0810, 107 (2008).
 - [27] A. V. Smirnov, Comput. Phys. Commun 189, 182 (2014).
 - [28] R. K. Ellis, G. Zanderighi, JHEP 0802, 002 (2008).
 - [29] H. H. Patel, Comput. Phys. Commun. 197, 276 (2015).
 - [30] T. Hahn and M. Perez-Victoria, Comput. Phys. Commun 118, 153 (1999).
 - [31] T. Hahn, Comput. Phys. Commun 168, 78 (2005).
 - [32] M. Beneke and V. A. Smirnov, Nucl. Phys. B 522, 321 (1998).

- [33] T. Kinoshita, J. Math. Phys. 3, 650 (1962).
- [34] T. D. Lee and M. Nauenberg, Phys. Rev. 133, B1549 (1964).
- [35] B. W. Harris and J. F. Owens, Phys. Rev. D 65, 094032 (2002).
- [36] M. Tanabashi et al. [Particle Data Group], Phys. Rev. D 98, 030001 (2018).
- [37] E. J. Eichten and C. Quigg, Phys. Rev. D 49, 5845 (1994).
- [38] <https://home.cern/news/news/accelerators/record-luminosity-well-done-lhc>.
- [39] J. R. Gaunt, C. H. Kom, A. Kulesza and W. J. Stirling, Eur. Phys. J. C 69, 53 (2010).
- [40] C. H. Chang and Y. Q. Chen, Phys. Rev. D 49, 3399 (1994).
- [41] X. C. Zheng, C. H. Chang, X. G. Wu, J. Zeng and X. D. Huang, arXiv: 1911.12531.